

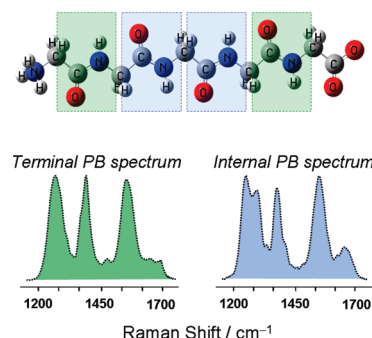
# UV Resonance Raman Elucidation of the Terminal and Internal Peptide Bond Conformations of Crystalline and Solution Oligoglycines

Sergei V. Bykov and Sanford A. Asher\*

Department of Chemistry, University of Pittsburgh, Pittsburgh Pennsylvania 15260

**ABSTRACT** Spectroscopic investigations of macromolecules generally attempt to interpret the measured spectra in terms of the summed contributions of the different molecular fragments. This is the basis of the local-mode approximation in vibrational spectroscopy. In the case of resonance Raman spectroscopy, independent contributions of molecular fragments require both a local-mode-like behavior and the uncoupled electronic transitions. Here, we show that the deep-UV resonance Raman spectra of aqueous solution-phase oligoglycines show independent peptide bond molecular fragment contributions, indicating that peptide bond electronic transitions and vibrational modes are uncoupled. We utilize this result to separately determine the conformational distributions of the internal and penultimate peptide bonds of oligoglycines. Our data indicate that in aqueous solution, the oligoglycine terminal residues populate conformations similar to those found in crystals ( $3_1$ -helices and  $\beta$ -strands) but with a broader distribution, while the internal peptide bond conformations are centered around the  $3_1$ -helix Ramachandran angles.

**SECTION** Kinetics, Spectroscopy



Spectroscopic methodologies are of a great importance in chemical analysis and for the determination of molecular structure. Interpretations of spectra generally use reductionist strategies whereby the spectrum of a macromolecule is first interpreted as the sum of the contributions of the individual molecular fragments. This first-order analysis is then reanalyzed to take into account higher-order phenomena such as the coupling of molecular dynamics between molecular fragments and the environment. For example, in UV resonance Raman (UVR) spectra of polypeptides, the vibrations could be localized within the individual peptide bond (PB), such that the PBs independently contribute. This would lead to spectra that are easily analyzed, where each PB vibration is not context-dependent. Alternatively, spectra of polypeptides may result from coupled motion of the backbone atoms of adjacent PBs.<sup>1</sup> This would lead to vibrational modes which depend upon their adjacent PB secondary structures.

Our previous study of a mainly ala-peptide in H<sub>2</sub>O/D<sub>2</sub>O mixtures indicated that the spectra of the partially deuterated chains could be roughly modeled (except for the amide I band) as a statistically weighted sum of deuterated and protonated independent segments.<sup>2,3</sup> This could only occur if the amide vibrations were essentially localized within the individual PB.

Here, we show that the deep-UV resonance Raman spectra of aqueous solution-phase oligoglycines show independent peptide bond molecular fragment contributions; the peptide bonds independently resonance Raman scatter. The peptide

bond electronic transitions and vibrational modes are uncoupled. We utilize this result to separately determine the conformational distributions of the internal and penultimate peptide bonds of oligoglycines.

**Vibrational and Electronic Coupling.** Figure 1 compares the 204 nm UVR difference spectrum between gly<sub>6</sub> and gly<sub>5</sub> to that of gly<sub>3</sub>. If there were negligible coupling between the PB vibrations, the gly<sub>3</sub> spectrum should closely approximate the two terminal PB spectra of oligopeptides, while the gly<sub>6</sub> – gly<sub>5</sub> spectrum should approximate a single internal PB vibration.

Summation of the gly<sub>6</sub> – gly<sub>5</sub> difference spectra and the gly<sub>3</sub> spectra essentially perfectly models the UVR spectra of gly<sub>5</sub> and gly<sub>6</sub> (Figure 1). The differences are below shot noise levels. This result indicates the lack of coupling of peptide bond vibrations between adjacent PB. The ability to accurately model the spectral intensities indicates that couplings between these vibrations and the resonant electronic transitions are localized within each PB.

**Internal PB Conformation Preferences.** The gly<sub>6</sub> – gly<sub>5</sub> spectrum differs significantly from that of gly<sub>3</sub>, with a clear doublet spanning the CH<sub>2</sub> twist/Am III spectral region, while gly<sub>3</sub> shows a single complex band shape. The CH<sub>2</sub> wagging, as well as the Am II and Am I bands of gly<sub>6</sub> – gly<sub>5</sub>, also differs from that of gly<sub>3</sub>, which may imply different structural preferences of the internal and terminal residues.

**Received Date:** October 11, 2009

**Accepted Date:** November 17, 2009

**Published on Web Date:** November 30, 2009

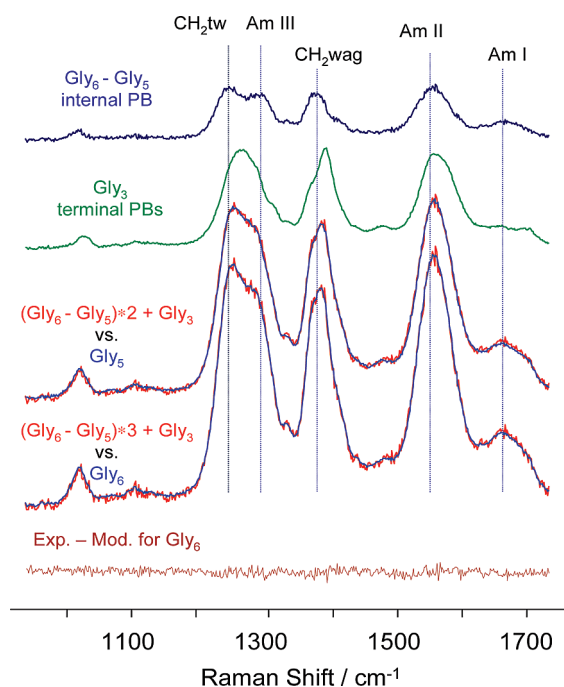


**Figure 1.** The 204 nm UVR spectra of oligoglycines in aqueous solutions containing 0.5 M LiClO<sub>4</sub> at neutral pH. The gly<sub>6</sub> – gly<sub>5</sub> difference spectrum approximates the spectrum of an internal peptide bond, while that of gly<sub>3</sub> approximates that of the two terminal peptide bonds. This is demonstrated by the fact that the summation of these spectra accurately models gly<sub>5</sub> and gly<sub>6</sub> spectra, as demonstrated by the lack of features in the bottom gly<sub>6</sub> difference spectrum between the experimental and modeled spectra. All of the UVRs were scaled relative to the internal standard perchlorate 932 cm<sup>–1</sup> band (not shown).

In a separate study reported elsewhere,<sup>4</sup> we compared the internal residue oligoglycine UVR spectra in solution to that of solid polyglycines of known conformations. These studies indicate that the internal PBs of oligoglycines occur as a broad ensemble of conformations centered around the  $\beta_1$ -extended helix conformation.

**Penultimate PB Conformation Preferences.** The UVR spectrum of gly<sub>3</sub> closely approximates the spectrum of the terminal PB of longer oligoglycines. Gly<sub>3</sub> shows a complex amide III band shape, suggesting that multiple conformational states of the peptide are populated in solution. Subtraction of the spectrum of an internal PB (gly<sub>6</sub> – gly<sub>5</sub>) from the spectrum of gly<sub>3</sub> produces a spectrum which is very similar to that of gly<sub>2</sub> in water (Figure 2), which should approximate the spectrum of the average of the two penultimate oligoglycine PBs.

We characterized the conformations of the gly<sub>3</sub> – (gly<sub>6</sub> – gly<sub>5</sub>) PB and gly<sub>2</sub> in solution by comparing their complex amide III bands to those of the amide III bands of crystalline gly<sub>2</sub> derivatives of known structures.

The solution UVR spectra of gly<sub>3</sub> – (gly<sub>6</sub> – gly<sub>5</sub>) and gly<sub>2</sub> show amide III spectral features similar to those in the spectra of gly<sub>2</sub> crystals with known  $\phi$  and  $\psi$  angles (Figure 2). These frequencies and bandwidths are listed in Table 1.

Crystalline Gly<sub>2</sub>·HCl·H<sub>2</sub>O have  $\phi = \pm 80^\circ$  and  $\psi = \pm 161^\circ$  dihedral angles that are close to those of a  $\beta_1$ -extended helix.<sup>5</sup> Crystals of Gly<sub>2</sub>·LiCl have  $\phi = \pm 154^\circ$  and  $\psi = \pm 168^\circ$ , which

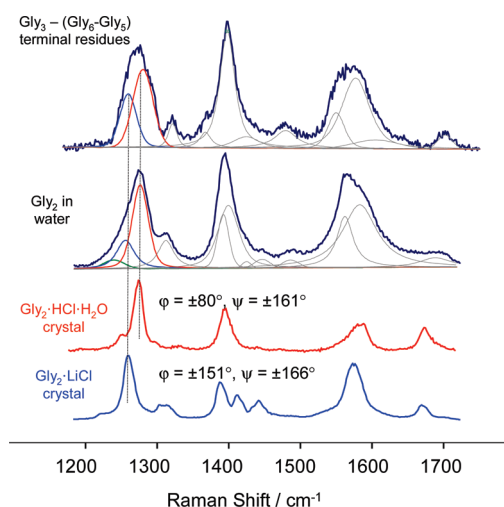


**Figure 2.** UVR difference spectrum gly<sub>3</sub> – (gly<sub>6</sub> – gly<sub>5</sub>) approximates the spectrum of the two terminal residues of oligoglycines in solution. Also shown is the spectra of gly<sub>2</sub> in solution and two gly<sub>2</sub> crystal samples of known structure, Gly<sub>2</sub>·HCl·H<sub>2</sub>O ( $\phi = \pm 80^\circ$ ,  $\psi = \pm 161^\circ$ ) and Gly<sub>2</sub>·LiCl ( $\phi = \pm 154^\circ$ ,  $\psi = \pm 168^\circ$ ).<sup>5,6</sup> The complex amide III band shapes of the solution samples can be well modeled with the amide III bands of these crystal gly<sub>2</sub> derivatives.

are close to that of a  $\beta$ -strand.<sup>6</sup> The amide III band of the  $\beta$ -strand gly<sub>2</sub> is 19 cm<sup>–1</sup> downshifted compared to that of the  $\beta_1$ -extended helix, indicating significant conformational sensitivity (Table 1). The amide III frequencies also depend upon the hydrogen bonding to the PB N–H since N–H bending significantly contributes to the amide III vibration. However both crystal structures have N–H hydrogen bonded to the Cl<sup>–</sup>, which implies similar HB strengths.

The amide III region of the gly<sub>3</sub>–(gly<sub>6</sub>–gly<sub>5</sub>) difference spectrum, as well as that of the gly<sub>2</sub> spectrum have a complex shape indicating significant conformational inhomogeneity of the terminal residues.

We can estimate the conformational distribution of the solution oligoglycine terminal residues by modeling the amide III region of the gly<sub>3</sub> – (gly<sub>6</sub> – gly<sub>5</sub>) difference spectrum with the well-defined amide III bands of crystal gly<sub>2</sub> of known structures. Assuming that the integrated intensities of the amide III bands are proportional to the populations of corresponding conformations in solution, we estimate that in solution, ~60% of terminal residues are in a  $\beta_1$ -extended helix-like conformation while ~40% are in extended  $\beta$ -strand-like conformation. Modeling of the gly<sub>2</sub> in solution gives similar results (~65% in a  $\beta_1$ -extended helix-like conformation and ~35% in an extended  $\beta$ -strand-like conformation).

As discussed above, the internal residues of oligoglycines in solution mainly populate a  $\beta_1$ -extended helix-like conformation. The higher preferences of the terminal residues for a  $\beta$ -strand conformation may result from the favorable interaction between terminal –NH<sub>3</sub><sup>+</sup> and the adjacent PB carbonyl, as well as between the terminal –COO<sup>–</sup> and the adjacent PB N–H, which are maximized for the completely extended conformation.

The amide III bands of the crystalline samples show full widths at half height of ~15–18 cm<sup>–1</sup>, which is likely to be their homogeneous bandwidth. The corresponding

**Table 1.** Frequencies ( $\nu$ ) and Bandwidths ( $w$ ) of UVRR Amide Bands in the  $\text{gly}_3 - (\text{gly}_6 - \text{gly}_5)$  Difference Spectrum,  $\text{gly}_2$  in Solution and  $\text{gly}_2$  Crystals

	$\text{gly}_3 - (\text{gly}_6 - \text{gly}_5)$ difference spectrum $\nu(w)/\text{cm}^{-1}$	$\text{gly}_2$ in solution $\nu(w)/\text{cm}^{-1}$	$\text{Gly}_2 \cdot \text{HCl} \cdot \text{H}_2\text{O}$ crystals $\nu(w)/\text{cm}^{-1}$	$\text{Gly}_2 \cdot \text{LiCl}$ crystals $\nu(w)/\text{cm}^{-1}$
Am III	1261(27), 1281(33)	1245(34), 1261(29), 1281(26)	1286(15)	1267(18)
$\text{CH}_2$ wag	1400(25)	1395(18), 1402(34)	1404(17)	1393(16)
Am II	1553(27), 1580(46)	1562(27), 1584(57)	1580(38), 1593(20)	1575(29)
Am I	1705(24)	1686(51)	1678(16)	1670(17)

solution amide III bands show almost two-fold broader bandwidths of  $\sim 26\text{--}34\text{ cm}^{-1}$ , which indicate that the terminal residues of oligoglycines in solution populate a broad ensemble of extended conformations with some preference for the  $3_1$ -helix.

In conclusion, the UV resonance Raman spectra of oligoglycines in aqueous solution can be accurately modeled as a linear sum of the spectra of their internal and terminal peptide bonds, which indicates the absence of vibrational and electronic coupling between adjacent PBs in polypeptides in solution. This result significantly simplifies polypeptide UVRR spectral analysis. The UVRR spectra of the oligoglycine internal PBs significantly differ from those of the terminal PBs, which implies different structural preferences. Our data indicates that in aqueous solution, oligoglycine terminal residues populate a broad range of extended conformations between  $3_1$ -helices and  $\beta$ -strands while the internal PBs conformation are centered around the Ramachandran angles of the  $3_1$ -helix.

## Experimental Methods

**Materials.**  $\text{Gly}_2$ ,  $\text{gly}_3$ ,  $\text{gly}_5$ , and  $\text{gly}_6$  were purchased from Bachem and used as received.  $\text{Gly}_2$  hydrochloride (Sigma Inc.) was recrystallized from water to obtain  $\text{Gly}_2 \cdot \text{HCl} \cdot \text{H}_2\text{O}$  crystals. Lithium chloride (T.J. Baker Inc.) was used for cocrystallization with  $\text{gly}_2$  to grow  $\text{Gly}_2 \cdot \text{LiCl}$  crystals. Lithium perchlorate (Fisher Scientific Inc.) was used to increase the solubility of  $\text{gly}_5$  and  $\text{gly}_6$  in water and as an internal Raman intensity standard.

**Raman Measurements.** For solution samples, we used 204 nm Raman excitation near the maximum absorbance of the peptide bond  $\pi \rightarrow \pi^*$  transition. The third harmonic of the Nd:YAG laser operating at 100 Hz was anti-Stokes Raman shifted in hydrogen to 204 nm (fifth anti-Stokes). The peptides were studied in a flow stream to avoid any contribution from photochemical degradation processes. Scattered light was dispersed by a double spectrometer and was detected by a Princeton Instruments Spec-10:400B CCD camera (Roper Scientific). A detailed description of the instrumentation is given elsewhere.<sup>7</sup> For solid samples, we used preresonance 229 nm excitation to minimize sample photo-degradation. Raman measurements were performed using an intracavity doubled Ar ion Laser (Coherent Inc.) A custom-made, rotating metal cell was used for the solid powder samples to avoid light-induced sample degradation. The crystal powder was pressed into a circular groove in the rotating metal cylinder. Typical accumulation times were less than 1 min.

## AUTHOR INFORMATION

### Corresponding Author:

\*To whom correspondence should be addressed. E-mail: asher@pitt.edu. Tel: 412 624-8570. Fax: 412 624-0588.

**ACKNOWLEDGMENT** We thank Dr. Steven Geib for X-ray crystal structure determinations and Bhavya Sharma for help in preparing this letter. This work was supported by the NIH, Grant 5R01EB002053.

## REFERENCES

- (1) Wang, Y.; Spiro, T. G. Vibrational and Electronic Couplings in Ultraviolet Resonance Raman Spectra of Cyclic Peptides. *Biophys. Chem.* **2003**, *105*, 461–470.
- (2) Mikhonin, A. V.; Asher, S. A. Uncoupled Peptide Bond Vibrations in  $\alpha$ -Helical and Polyproline II Conformations of Polyalanine Peptides. *J. Phys. Chem. B* **2005**, *109*, 3047–3052.
- (3) Mix, G.; Schweitzer-Stenner, R.; Asher, S. A. Uncoupled Adjacent Amide Vibrations in Small Peptides. *J. Am. Chem. Soc.* **2000**, *122*, 9028–9029.
- (4) Bykov, S. V.; Asher, S. A. Conformation of Polyglycine in Solution. In preparation.
- (5) Parthasarathy, R. Crystal Structure of Glycylglycine Hydrochloride. *Acta Crystallogr., Sect. B* **1969**, *25*, 509–518.
- (6) Mueller, G.; Maier, G.-M.; Lutz, M. Lithium Coordination to Amino Acids and Peptides. Synthesis, Spectroscopic Characterization and Structure Determination of Lithium Complexes of Neutral and Anionic Glycine and Diglycine. *Inorg. Chim. Acta* **1994**, *218*, 121–131.
- (7) Bykov, S.; Lednev, I.; Ianoul, A.; Mikhonin, A.; Munro, C.; Asher, S. A. Steady-State and Transient Ultraviolet Resonance Raman Spectrometer for the 193–270 nm Spectral Region. *Appl. Spectrosc.* **2005**, *59*, 1541–1552.